Case Studies in Thermal Engineering 21 (2020) 100660

Contents lists available at ScienceDirect

Case Studies in Thermal Engineering

journal homepage: http://www.elsevier.com/locate/csite

Hybrid nanofluid on mixed convective radiative flow from an irregular variably thick moving surface with convex and concave effects

Umair Khan [a], Anum Shafiq [b], A. Zaib [c,*], Dumitru Baleanu [d,e,f]

[a] Department of Mathematics and Social Sciences, Sukkur IBA University, Sukkur, 65200, Sindh, Pakistan
[b] School of Mathematics and Statistics, Nanjing University of Information Science and Technology, Nanjing, 210044, China
[c] Department of Mathematical Sciences, Federal Urdu University of Arts, Science & Technology, Gulshan-e-Iqbal, Karachi, 75300, Pakistan
[d] Department of Mathematics, Cankaya University, 06790, Ankara, Turkey
[e] Institute of Space Sciences, 077125, Magurele, Romania
[f] Department of Medical Research, China Medical University Hospital, China Medical University, Taichung, 40447, Taiwan

ARTICLE INFO

Keywords:
Dual solutions
Shrinking/stretching surface
Nanofluid
Thermal radiations
MHD
Mixed convection

ABSTRACT

The analysis explores the significance of thermal radiation on mixed convective boundary layer flow of a hybrid (SiO_2–MoS_2/H_2O) nanofluid. The permeability of the stretched/shrinking surface is allowing the wall fluid suction, whereas radiation phenomenon is also incorporated in the presence of thermal convection. The combination of SiO_2 nanoparticles and MoS_2/H_2O nanofluid are being modeled using the analytical nanofluid hybrid model in the present work. The hybrid nanofluid governing equations are transformed utilizing the similarity transformation technique. The transformed boundary value problem, then solved by bvp4c technique in MATLAB software. For specified values of various parameters the numerical results are obtained. The findings indicate dual solutions, up to some amount of stretching/shrinking parameter. The suction parameter decelerates the friction factor and accelerates the heat transfer rate. Also, the temperature augments due to the radiation and nanoparticles volume fraction in both solutions, whereas the velocity declines due to nanoparticles volume fraction.

1. Introduction

Many innovative methods have been used in recent decades to increase heat transfer rate to attain various rates of thermal abilities. To do this, it is very important to enhance thermal conductivity. Eventually, many attempts have been made to disperse larger thermal conductive solid materials into the fluids to improve thermal conductivity. Since the early 1990s nanofluids have come into being. To meet the requirements of industrial applications, several nanofluid studies have been conducted.

Despite the fact that nanofluids fulfill the thirst of researchers/specialists in thermal efficiency even today a better type of liquid is still in pursuit. In dealing with these, advanced nanofluid forms like "hybrid nanofluid" have emerged with a high thermal conductivity compared to nanofluid. The present research therefore focuses mainly on utilizing of hybrid nanofluid, which is the authors' fundamental aim of improving the rate of heat transfer.

The inexpensive, improved fluidness and long-term firmness are three major requirements for nanofluid for real-world heat transfer

* Corresponding author.
E-mail address: aurangzaib@fuuast.edu.pk (A. Zaib).

https://doi.org/10.1016/j.csite.2020.100660
Received 15 April 2020; Received in revised form 12 May 2020; Accepted 16 May 2020
Available online 21 May 2020

Nomenclature

A, b	Constants
B_0	Magnetic field strength (Kg $s^{-2}A^{-1}$)
C_f	Skin friction coefficient
c_p	Specific heat (J Kg^{-1} K^{-1})
f	Dimensionless velocity
g	Gravity acceleration (m s^{-2})
Gr_x	Grashof number
k^*	Mean absorption coefficient
k	Thermal conductivity (W $m^{-1}K^{-1}$)
M	Magnetic number
m	Shape parameter
Nu_x	Nusselt number
Pr	Prandtl number
q_r	Radiative heat flux (W m^{-2})
R_d	Radiation parameter
Re_x	Local Reynolds number
S	Suction parameter
T_1	Temperature (K)
T_w	Wall temperature (K)
T_∞	Ambient temperature (K)
Θ	Dimensionless temperature
(u_1, v_1)	Velocity components (ms^{-1})
U_0	Stretching velocity (ms^{-1})
U_∞	Free stream velocity (ms^{-1})
v_w	mass flux velocity
(x, y)	Cartesian coordinates (m)

Greek Symbols

α	thermal diffusivity (m^2 s^{-1})
β	Thermal expansion (K^{-1})
ε	Wall thickness parameter
λ	Stretching/Shrinking parameter
μ	dynamic viscosity (Pa s)
φ	The volume fraction of nanoparticles
ν_f	Kinematic viscosity of the base fluid (m^2 s^{-1})
ρ	density (Kg m^{-3})
σ^*	Stefan–Boltzmann constant
σ	The electrical conductivity (Sm^{-1})
(ρc_p)	Heat capacity (J m^{-3} K^{-1})
ψ	Stream function
η	Similarity variable

Subscripts

f	Base fluid
s_1,s_2	Solid nanoparticles
nf	Nanofluid
hnf	Hybrid nanofluid
w	Wall boundary condition
∞	Free-stream condition

Superscripts

‘	Derivative w.r.t. η

applications. Several researchers have recently used oxide nanomaterials to replace metal and carbon nanomaterials in large-scale processing. Regrettably, oxide nanomaterials thermal conductivity is lower than that of metal nanomaterials, and solving the lofty volume fraction suspension of oxide materials (>5.0 vol. percent) is necessary to accomplish the thermal conductivity improvement needed. The only way to sustain good fluidity is to decrease the particle concentration. Oxiding materials, in particular, cannot meet the basic requirements and the development of new low costs and high performance, nanomaterials is still the most imperative

challenge in the nanofluid field. Wakif et al. [1] employed the non-homogenous model of Buongiorno to examine the H_2O based metallic nanomaterials b/w two infinite plates. Sheikholeslami et al. [2] discussed the influence of nanometer size particle and fins by considering different shapes via a heat exchanger and obtained the results by utilizing Galerkin FEM. The time dependent free convective flow from a vertical heated plate was discussed by Wakif et al. [3]. Wakif et al. [4] deliberated the meta-analysis on the importance of either tiny or nano materials rendering to force of thermophoretic during the substances of liquid dynamics due to temperature-gradient. The impact of flow rate, flattened percentage, CuO mass fraction and vapor quality are experimentally investigated by Sheikholeslami et al. [5]. Nayak et al. [6] scrutinized the mixed convective flow of water based metallic oxide and metallic nanomaterials through a thin needle. Sheikholeslami et al. [7] has been designed the unit of the storage of clean energy to reduce the consumption of energy via the building by applying the nanoparticles and porous media. The time dependent 3D radiative flow containing Casson liquid assigning tiny materials was explored by Thumma et al. [8]. Recently, Zaib et al. [9] examined the impact of radiation and magnetic function on flow of non-Newtonian blood nanofluid comprising magnetic ferroparticles with mixed convection.

A new form of hybrid nanoliquid is used to make it economical. Inserting small metal nanomaterials/nanotubes amounts into an oxide/metal nanostructure now immersed in a base liquid will unforeseenly increase the thermal properties. The qualities of "hybrid nanofluid" are large proficient thermal conductivity, solidness, upgraded heat exchange, and recognized to inordinate perspective proportion, benefits and disadvantages of separate suspension and synergistic impression of the nanostructure. The high thermal conductivity of nanofluid is changed into the improvement of vitality productivity, low working costs and way better execution.

Hybrid nanofluids have wide range of usages in most of heat transfer fields like generator cooling, biomedical, the nuclear system cooling, electronic cooling, transformer cooling, solar heating, thermal storage, lubrication, welding, construction cooling and ventilation, alcohol control, protection, heat pump, refrigeration, spacecraft and aircraft. Hybrid nanofluids implementation within the industry is important because they have better performance than nanofluid. Such features fascinated many researchers working towards hybrid nanofluid. Several experimental inspections have provided incredible outcomes from the utilization of such sorts of hybrid nanofluid systems. Niihara [10] outlined nano composites, which upgraded mechanical and thermal properties through an unused conception of substantial design. Jana et al. [11] made extensive advances in fluid thermal conductivity by presenting single- and hybrid nano additives. Suresh et al. [12] conducted an examination to synthesize hybrid nanofluid. The nanocomposites produced had a new nanostructure concept, and enhanced dramatically thermal and mechanical properties. Momin [13] investigated the experimental learning of laminar mixed convection flow of hybrid nanofluid in inclined tube. Afterward, Suresh et al. [14] analyzed affect of hybrid ($Al_2O_3 - Cu$ = water) nanofluid in heat exchange. Baghbanzadeh et al. [15] inspected the amalgamation of hybrid nanoparticles of multi/spherical silica divider carbon nanotubes and thermal conductivity of the related nanofluids.

Recently, researchers have focused to study hybrid nanofluids problems numerically. Few articles are discussed here. Khashi'ie et al. [16] examined coupled impacts of thermally stratified mixed convective flow and rate of transfer of heat, comprising hybrid $Cu–Al_2O_3$/water nanofluid. Lund et al. [17] analyzed the duality and stability investigation of a magneto-hydrodynamics flow of hybrid nanofluid towards a shrinking/stretching surface. Wakif et al. [18] utilized the modified Buongiorno model to inspect the hybrid nanofluid containing copper-alumina nanoparticles with surface roughness and radiation effects.

Thermal radiation (TR) impact is significantly essential at large operating temperature, and cannot be neglected. Several engineering procedures happen at extreme temperatures and thus TR awareness plays a significant role in layout of relevant apparatus. It has also some major role in many industrial usages like furnace design and glass production and moreover, in space innovation applications, such as space vehicles, propulsion systems, comical flight aerodynamics rocket, spacecraft and plasma physics, combustion processes, within the stream structure of nuclear plants, internal combustion engines, solar radiations and ship compressors. Considering these, few scholars have prepared commitments for the examination of MHD nanofluid stream with TR phenomenon. Khan et al. [19] displayed a similar examination of time independent two dimensional flow of a nanofluid over an extending radiative plate with impact of magnetic phenomena. Poornima and Reddy [20] examined numerically the simultaneous consequences of thermal radiation and magnetic phenomena on nanoliquid flow towards a nonlinear stretched surface. Mat [21] theoretically investigated magneto-hydrodynamic mixed convective flow of a radiative vertical stretched heated surface in a power law nanoliquid. Shateyi et al. [22] investigated the significance of MHD boundary layer nanofluid flow towards a moving surface with radiation effect. The impact of MHD and radiation heat flow of nanofluid along a stretched plate with velocity slip and convective boundary conditions was examined by Reddy [23]. Shankar and Haile [24] analyzed simultaneously the significance of magnetic, viscous dissipation, thermal radiation and permeability of surfaces on heat transfer of nanofluid towards a moving flat surface. Several investigations are also in literature, see Ref. [25–30].

The foregoing literature review discloses that the general problem of mixed convection containing hybrid nanofluids with an erratic variable thickness and particularly concave and convex effects have been underlined as mostly unexplored fields. Therefore, the current study accentuates the mixed convective flow of hybrid ($SiO_2–MoS_2/H_2O$) nanoliquid towards an irregular variable permeable shrinking/stretching sheet with concave and convex effects. Also, the radiation and magnetic phenomena are invoked. The differential system of equations is obtained by using similarity phenomenon and solved using the bvp4c numerical technique [31–34]. Also, our concern about the appearance of the non-unique solution of the present study.

The organization of the manuscript is as follows:

2. Problem formulation

The current inquiry focuses on a theoretical analysis on the magneto radiative flow with heat transfer of water based hybrid $SiO_2–MoS_2$ nanoparticles through a shrinking/stretching surface under mixed convection (see Fig. 1). The surface thickness is

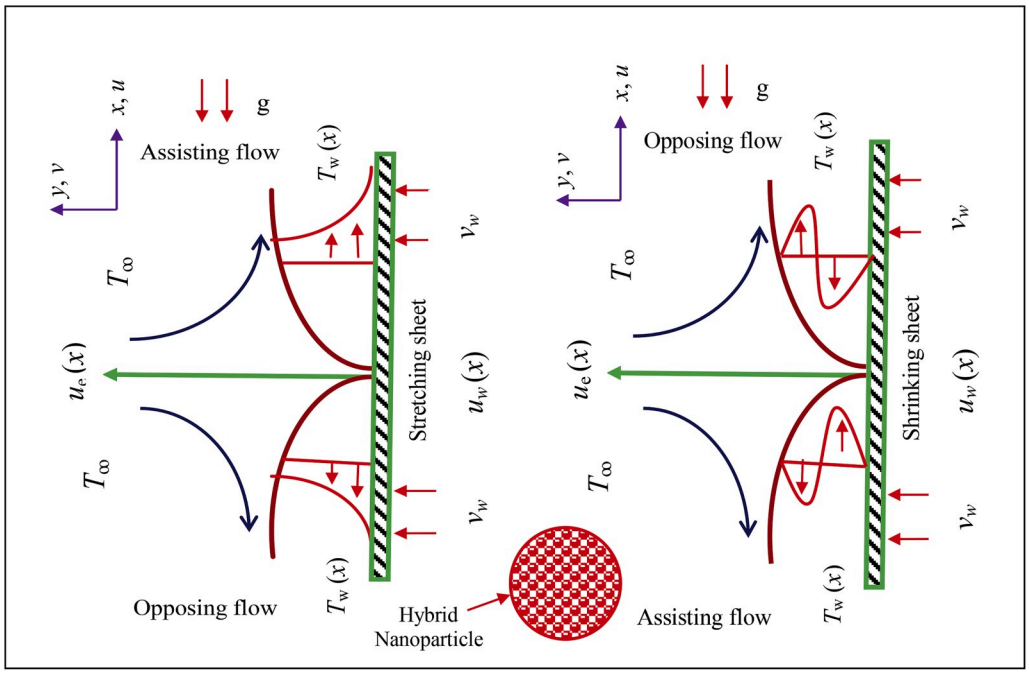

Fig. 1. Diagram of the problem.

considered as $y = A(x+b)^{\frac{1-m}{2}}$. It is presumed that for 2D stagnation point, the shrinking/stretching nonlinear velocity is $y = A(x+b)^{\frac{1-m}{2}}$ with A is constant, and the ambient velocity is $U_\infty(x+b)^m$, where U_∞ is constant and m is the shape parameter used for controlling the surface shape. In addition, the magnetic effect is taken in the variable form as $B = B_0(x+b)^{\frac{m-1}{2}}$, while the temperature of wall inside the region of boundary-layer is considered to be $T_w(x)$ and the fixed value at far away from the sheet is signified as T_∞. In addition, the mass flux velocity is considered as $v_w(x) = (v_0(x+b)^{m-1})^{0.5}$ where the negative and positive value of $v_w(x)$ indicates to suction and blowing, respectively. The leading PDEs based on the above assumptions can be patterned as

$$\frac{\partial v_1}{\partial y} + \frac{\partial u_1}{\partial x} = 0, \tag{1}$$

$$v_1\frac{\partial u_1}{\partial y} + u_1\frac{\partial u_1}{\partial x} - u_e\frac{du_e}{dx} = \frac{\mu_{hbnf}}{\rho_{hbnf}}\left(\frac{\partial^2 u_1}{\partial y^2}\right) - \frac{\sigma_{hbnf}B^2}{\rho_{hbnf}}(u_1 - u_e) + g\frac{(\rho\beta)_{hbnf}}{\rho_{hbnf}}(T_1 - T_\infty), \tag{2}$$

$$v_1\frac{\partial T_1}{\partial y} + u_1\frac{\partial T_1}{\partial x} = \alpha_{hbnf}\left(\frac{\partial^2 T_1}{\partial y^2}\right) - \frac{1}{(\rho c_p)_{hbnf}}\frac{\partial}{\partial y}(q_r), \tag{3}$$

The suitable boundary conditions are

$$\begin{aligned} &u_1 = U_0(x+b)^m = u_w(x), \quad v_1 - v_w = 0, \quad T_1 = T_\infty + (x+b)^{2m-1} = T_w(x) \ \text{ at } \ y = A(x+b)^{\frac{-m+1}{2}}, \\ &u_1 = U_\infty(x+b)^m = u_e(x), \quad T_1 \to T_\infty \ \text{ as } \ y \to \infty. \end{aligned} \tag{4}$$

where (v_1, u_1) scrutinized the components velocity in the respectively $y-$ and $x-$ directions, $(\mu_{hbnf}, \rho_{hbnf})$ signifies the hybrid viscosity and density, respectively, T_1 the temperature, q_r the radiative heat flux, $((\rho\beta)_{hbnf}, (\rho c_p)_{hbnf})$ denotes the hybrid thermal expansion coefficient and heat capacity, respectively and $(\alpha_{hbnf}, \sigma_{hbnf})$ the thermal diffusivity and electrical conductivity of hybrid nanofluid, respectively.

2.1. Thermo-physical properties of hybrid nanofluid

Mixing of hybrid nanofluid in water based convectional fluid comprising $SiO_2(\varphi_1)$ and $MoS_2(\varphi_2)$ nanomaterials. Furthermore, the SiO_2 volume fraction of nanoparticles was set at 1% and MoS_2 ranges from 1 to 5%. The volume fraction of hybrid nanofluid is suggested according to Xie et al. [35] as

Table 1 presents the features of thermo-physical of hybrid nanofluid. Whereas the values of the thermo-physical characteristics of base fluid and hybrid nanofluid are illustrated in Table 2.

Table 1
Thermo physical attributes of hybrid nanofluid [36].

Properties	Hybrid nanofluid
Dynamic viscosity	$\mu_{hbnf} = \frac{\mu_f}{(1-\varphi_1)^{2.5}(1-\varphi_2)^{2.5}}$
Density	$\rho_{hbnf} = [\varphi_2\rho_{s_2} + (1-\varphi_2)\{\varphi_1\rho_{s_1} + (1-\varphi_1)\rho_f\}]$
Thermal conductivity	$k_{hbnf} = \frac{(k_{s_2}+2k_{nf}) - 2\varphi_2(k_{nf}-k_{s_2})}{(k_{s_2}+2k_f) + \varphi_2(k_{nf}-k_{s_2})} \times k_{nf}$ with $k_{nf} = \frac{(2k_f+k_{s_1}) - 2\varphi_1(k_f-k_{s_1})}{(2k_f+k_{s_1}) + \varphi_1(k_f-k_{s_1})} \times k_f$
Electrical conductivity	$\sigma_{hbnf} = \sigma_{bf}\left[\frac{\sigma_{s_2}(1+2\varphi_2) + 2\sigma_{bf}(1-\varphi_2)}{\sigma_{s_2}(1-\varphi_2) + \sigma_{bf}(2+\varphi_2)}\right]$ with $\sigma_{bf} = \sigma_f\left[\frac{\sigma_{s_1}(1+2\varphi_1) + 2\sigma_f(1-\varphi_1)}{\sigma_{s_1}(1-\varphi_1) + \sigma_f(2+\varphi_1)}\right]$
Thermal expansion coefficient	$(\rho\beta)_{hbnf} = [\varphi_2(\rho\beta)_{s_2} + (1-\varphi_2)\{\varphi_1(\rho\beta)_{s_1} + (1-\varphi_1)(\rho\beta)_f\}]$
Heat capacitance	$(\rho c_p)_{hbnf} = [(1-\varphi_2)\{\varphi_1(\rho c_p)_{s_1} + (1-\varphi_1)(\rho c_p)_f\} + \varphi_2(\rho c_p)_{s_2}]$

Table 2
The thermo physical features of regular fluid and nanoparticles [37–39].

Properties\constituents	Water	MoS_2	SiO_2
c_p(J/kg K)	4179	397.746	730
k (W/m K)	0.613	34.5	1.5
ρ (kg/m_3)	997.1	5060	2650
$\sigma(\Omega.m)^{-1}$	0.05	2.09×10^4	1.0×10^{-18}
β (1/K)	21	2.8424×10^{-5}	42.7

Here, φ the volume fraction of nanoparticle, while the other symbols for the base fluid and hybrid nanofluids comprising in Table 1, respectively studied namely like μ_f the absolute viscosity, (ρ_s, ρ_f) the densities, (k_s, k_f) the thermal conductivities, $((\rho c_p)_f, (\rho c_p)_s)$ the heat capacitances, and as well as (σ_s, σ_f) the electrical conductivities.

By employing the Rosseland estimation for the radiative heat flux, we have

$$q_r = -\frac{4\sigma^*}{3k^*}\frac{\partial {T_1}^4}{\partial y}, \tag{5}$$

where σ^* and k^* represent the Stefan Boltzmann constant and the mean absorption coefficient, respectively.

After using the Taylor series approximation for ${T_1}^4$ centered around T_∞ and ignoring the terms involving the higher-order, we get

$${T_1}^4 \approx -3T_\infty^4 + 4T_\infty^3 T_1. \tag{6}$$

The surface position resolutely depends on m. It is worthy of mention that the sheet becomes flat when $m = 1$; the thickness of the wall will increases for m less than one and the shape of the sheet occurs to the outer convex type and decays for m greater than one and as a result, the shape becomes the type of inner concave.

The values of m are also responsible for the type of motion, i.e. $m$equal to zero, the movement is linear with steady velocity. Moreover, the motion is decelerated for $m-1<0$ and accelerated for$m-1>0$.

Employing the similarity variables as

$$\zeta = y\left(\frac{U_\infty(x+b)^{m-1}}{2\nu_f}(m+1)\right)^{0.5}, \quad u_1 = U_\infty(x+b)^m g'(\zeta), \Theta(\zeta) = \frac{T_1 - T_\infty}{T_w - T_\infty},$$
$$v_1 = -\left(\frac{m+1}{2}\nu_f U_\infty(x+b)^{m-1}\right)^{0.5}\left[g + \zeta g', \frac{m-1}{m+1}\right]. \tag{7}$$

Utilizing Eq. (7) through the well-known Eq. (5), Eqs. (2)–(4) transmuted into ODE's in the following form:

$$\frac{g'''}{\Omega_a} + \Omega_b\left(gg'' + \frac{2m}{m+1}\left(1-g'^2\right)\right) + \left(\frac{2}{m+1}\right)\{M\Omega_c(1-g') + \Omega_d\xi\Theta\} = 0, \tag{8}$$

$$\Theta''\left[\frac{k_{hbnf}}{k_f} + \frac{4}{3}R_d\right] + \Pr\Omega_e\left(g\Theta' - \left(\frac{4m-2}{m+1}\right)\Theta g'\right) = 0. \tag{9}$$

$$g'(\varepsilon)=\lambda, g(\varepsilon)=S+\varepsilon\frac{1-m}{m+1}, \Theta(\varepsilon)=1 \ \text{ at } \ \varepsilon=A\sqrt{\frac{U_\infty(m+1)}{2\nu_f}},$$
$$g'(\infty)\to 1, \Theta(\infty)\to 0 \ \text{ at } \ \varepsilon\to\infty. \tag{10}$$

where $\varepsilon=A\sqrt{\frac{(m+1)U_\infty}{2\nu_f}}$ and $S=-\sqrt{\frac{v_0}{(m+1)U_\infty\nu_f}}$ is the wall thickness and mass suction parameter, respectively.

In which:

$$\Omega_a=(1-\varphi_1)^{2.5}(1-\varphi_2)^{2.5},$$
$$\Omega_b=\left(\varphi_2\frac{\rho_{s_2}}{\rho_f}+(1-\varphi_2)\left\{(1-\varphi_1)+\varphi_1\frac{\rho_{s_1}}{\rho_f}\right\}\right)$$
$$\Omega_c=\left(\frac{\sigma_{s_2}(1+2\varphi_2)+2\sigma_f\left\{\frac{\sigma_{s_1}(1+2\varphi_1)+2\sigma_f(1-\varphi_1)}{\sigma_{s_1}(1-\varphi_1)+\sigma_f(2+\varphi_1)}\right\}(1-\varphi_2)}{\sigma_{s_2}(1-\varphi_2)+\sigma_f\left\{\frac{\sigma_{s_1}(1+2\varphi_1)+2\sigma_f(1-\varphi_1)}{\sigma_{s_1}(1-\varphi_1)+\sigma_f(2+\varphi_1)}\right\}(2+\varphi_2)}\right)\left(\frac{\sigma_{s_1}(1+2\varphi_1)+2\sigma_f(1-\varphi_1)}{\sigma_{s_1}(1-\varphi_1)+\sigma_f(2+\varphi_1)}\right), \tag{11}$$
$$\Omega_d=\left((1-\varphi_2)\left[(1-\varphi_1)+\varphi_1\frac{(\rho\beta)_{s_1}}{(\rho\beta)_f}\right]+\varphi_2\frac{(\rho\beta)_{s_2}}{(\rho\beta)_f}\right),$$
$$\Omega_e=\left((1-\varphi_2)\left[\varphi_1\frac{(\rho c_p)_{s_1}}{(\rho c_p)_f}+(1-\varphi_1)\right]+\varphi_2\frac{(\rho c_p)_{s_2}}{(\rho c_p)_f}\right),$$

Now substituting

$$g(\zeta)=f(\eta)=f(\zeta-\varepsilon) \tag{12}$$

In one form of variable, the concluding equations are specified as:

$$\frac{f'''}{\Omega_a}+\Omega_b\left(ff''+\frac{2m}{m+1}\left(1-f'^2\right)\right)+\left(\frac{2}{m+1}\right)\{M\Omega_c(1-f')+\Omega_d\xi\theta\}=0 \tag{13}$$

$$\theta''\left[\frac{k_{hbnf}}{k_f}+\frac{4}{3}R_d\right]+\Pr\Omega_e\left(f\theta'-\left(\frac{4m-2}{m+1}\right)\theta f'\right)=0 \tag{14}$$

The boundary restriction levied is

$$f'(0)=\lambda, f(0)-S=\varepsilon\frac{1-m}{m+1}, \theta(0)=1 \ \text{ at } \ \eta=0,$$
$$f'(\infty)\to 1, \theta(\infty)\to 0 \ \text{ at } \ \eta\to\infty. \tag{15}$$

The non-dimensional factors in Eqs. 12–14 which is mathematically expressed as:

$$\xi=\frac{Gr_x}{\mathrm{Re}_x^2}, M=\frac{\sigma_f B_0{}^2}{\rho_f U_\infty}, \mathrm{Re}_x=\left(\frac{U_w(x+b)}{\nu_f}\right), \Pr=\frac{\nu_f}{\alpha_f}, Gr_x=\frac{g\beta_f(T_w-T_\infty)(x+b)^3}{\nu_f^2}, \lambda=\frac{U_0}{U_\infty},$$

$$R_d=\frac{4\sigma^* T_\infty^3}{k_f k^*}.$$

While showing their proper names of the above-mentioned parameters, called the mixed convective parameter (ξ) (where it is mathematically written as $\xi=Gr_x/\mathrm{Re}_x^2$ called the fraction of (Gr_x) Grashof and Reynolds number (Re_x), radiation parameter (R_d) magnetic parameter (M), and the Prandtl number $(\Pr)$.

The local Nusselt and the skin friction factor are the physical significant quantities concerning on the flow with heat transport. These quantities in the ODEs form are

$$Nu_x=\frac{-x}{k_f(T_w-T_\infty)}\left(k_{hbnf}\frac{\partial T_1}{\partial y}+\frac{4\sigma^*}{3k^*}\frac{\partial T_1{}^4}{\partial y}\right)\Big|_{y=A(x+b)^{\frac{1-m}{2}}} \tag{16}$$

$$C_f=\frac{\mu_{hbnf}}{\rho u_e^2(x)}\left(\frac{\partial u_1}{\partial y}\right)_{y=A(x+b)^{\frac{1-m}{2}}} \tag{17}$$

Applying (7), we get

$$(\mathrm{Re}_x)^{\frac{-1}{2}}Nu_x=-\left\{\frac{k_{hbnf}}{k_f}+\frac{4}{3}R_d\right\}\left\{\frac{m+1}{2}\right\}^{\frac{1}{2}}\theta'(0) \tag{18}$$

Table 3
The comparison values of $(\mathrm{Re}_x)^{0.5}C_f$ and $(\mathrm{Re}_x)^{-0.5}Nu_x$ for the buoyancy assisting flow $\xi = 1$, while the rest of the parameters are: $S = m = 1, \varphi_1 = \varphi_2 = R_d = M = 0$.

Pr	$(\mathrm{Re}_x)^{0.5}C_f$		$(\mathrm{Re}_x)^{-0.5}Nu_x$	
	Mahapatra and Gupta [40]	Present results	Nazar et al. [41]	Present results
0.72	0.3645	0.364548	1.0931	1.093178
6.8	0.1804	0.180458	3.2902	3.290242
20	0.1175	0.117583	5.6230	5.623029
40	0.0873	0.08730	7.9463	7.946312
60	0.0729	0.072956	9.7327	9.732745
80	0.0640	0.064045	11.2413	11.241387
100	0.0578	0.057829	12.5726	12.572643

Table 4
The comparison values of $(\mathrm{Re}_x)^{0.5}C_f$ and $(\mathrm{Re}_x)^{-0.5}Nu_x$ for the buoyancy opposing flow $\xi = -1$, while the rest of the parameters are $S = m = 1, \varphi_1 = \varphi_2 = R_d = M = 0$.

Pr	$(\mathrm{Re}_x)^{0.5}C_f$		$(\mathrm{Re}_x)^{-0.5}Nu_x$	
	Mahapatra and Gupta [40]	Present results	Nazar et al. [41]	Present results
0.72	-0.3852	-0.385229	1.0293	1.029350
6.8	-0.1804	-0.180446	3.2466	3.246652
20	-0.1183	-0.118306	5.5923	5.592340
40	-0.0876	-0.087609	7.9227	7.922785
60	-0.0731	-0.073145	9.7126	9.712655
80	-0.0642	-0.064266	11.2235	11.223545
100	-0.0579	-0.057932	12.5564	12.556475

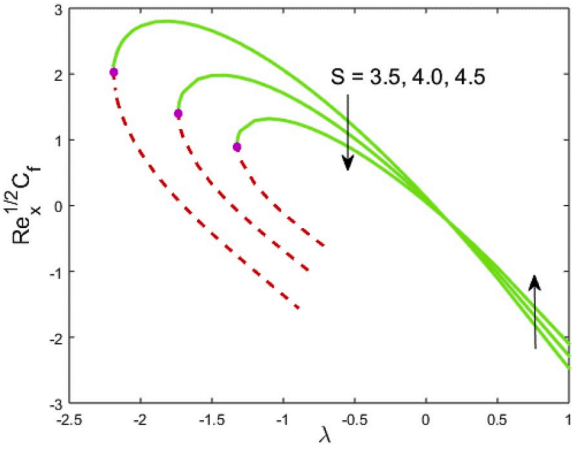

Fig. 2. Impact of *S*on $Re_x{}^{1/2}C_f$.

$$\sqrt{\mathrm{Re}_x}C_f = \frac{f''(0)}{(1-\varphi_1)^{2.5}(1-\varphi_2)^{2.5}}\left\{\frac{m+1}{2}\right\}^{\frac{1}{2}} \tag{19}$$

where $\mathrm{Re}_x = \frac{U_w(x+b)}{\nu_f}$ is the Reynolds number.

3. Results and discussion

The altered model in the ODEs (13) and (14) form with restricted condition (15) can be worked out numerically through bvp4c solver based on collocation technique. The current numerical technique is tested through a comparison via the results achieved by Mahapatra and Gupta [40] and Nazar et al. [41] in Tables 3 and 4. The current results are observed in tremendous agreement with outcomes of [40,41]. The following fixed parameters $M = 0.1, \xi = -0.1, \lambda = -1, S = 5, m = 0.5, \varepsilon = 0.1, R_d = 0.1,$ and $\mathrm{Pr} = 6.2$ are taken throughout the investigation.

Illustration of the friction factor and the heat transfer for the change values of suction *S* versus λ are deployed in Figs. 2 and 3,

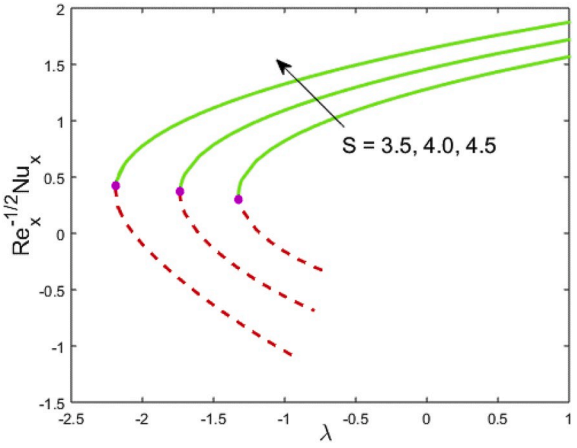

Fig. 3. Impact of $SonRe_x^{-1/2}Nu_x$.

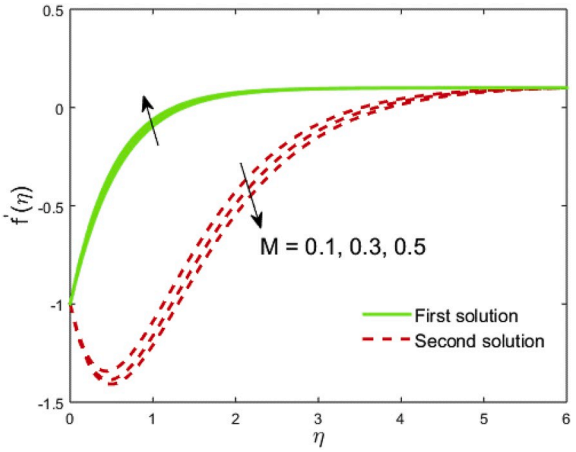

Fig. 4. Impact of M on $f'(\eta)$.

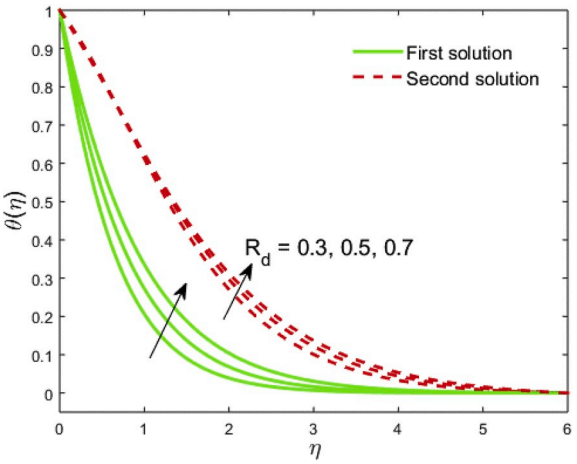

Fig. 5. Impact of R_d on $\theta(\eta)$.

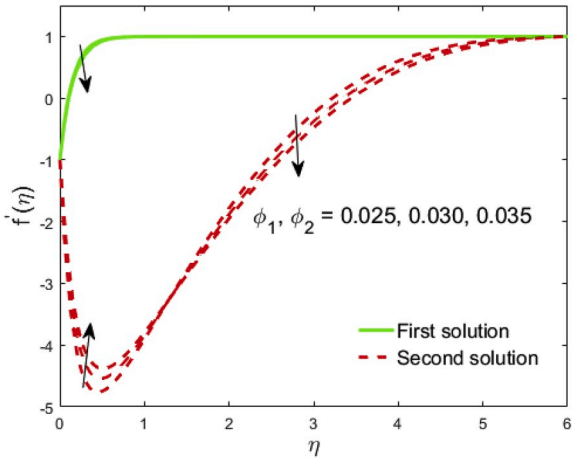

Fig. 6. Impact of φ_1, φ_2 on $f'(\eta)$.

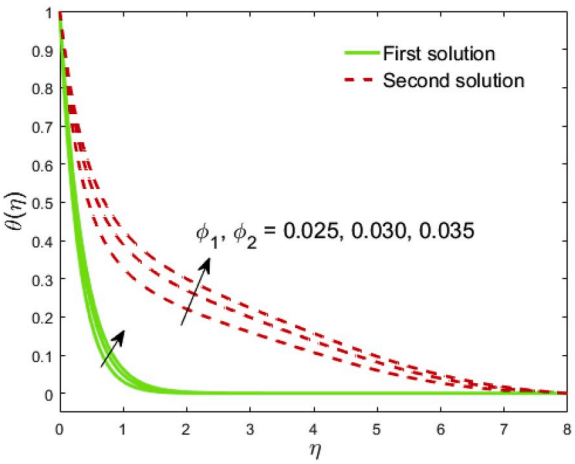

Fig. 7. Impact of φ_1, φ_2 on $\theta(\eta)$.

respectively. In these graphs, the dash lines and solid lines signify the second (lower branch) and first (upper branch) solutions, respectively. Also, these portraits reveal that the upper and lower branch solutions overlap at some preset value of λ recognized as a critical values λ_c which is highlighted with red dot. The multiple or dual results are accomplished in the opposing flow, while the single result is obtained in the assisting flow. In addition, there is certainly a critical value λ_c for each chosen value of S for which the result exists. Derived from our calculation, we scrutinize that $\lambda_c = -2.3956, -1.7542, -1.3985$, respectively for $S = 3.5, 4, 4.5$. It is noted here that the values of $|\lambda_c|$ reduce due to suction parameter. Therefore, the suction parameter is to accelerate the variety of λ for which result exists. Moreover, Fig. 2 demonstrates that the friction factor initially enhances due to S and then declines in the first and second solutions, whereas, Fig. 3 suggests that in the first branch solution (FBS) the transfer rate of heat increases and shrinks in the second branch solution (SBS). Physically, the surface permeability catches slower moving molecules and shrinks the surface thermal conductivity which consequently increases the heat transfer rate.

The magnetic field impact on the velocity is shown in Fig. 4. Fig. 4 explains that the velocity boost up due to M in FBS and shrinks in the SBS outcomes. Physically, the magnetic number augments the fluid motion within the boundary-layer plus in Eq. (2), that stay progressive in the constituency. Also, the magnetic influence of the fluid enhances the Lorentz force and has a propensity to expedite the motion of nanofluid in the region of boundary. The effect of radiation parameter R_d on the temperature is sketched in Fig. 5. Fig. 5 suggests that the temperature distribution as expected upsurges in the first and second branch solutions. The fact behind this that the sheet heat flux enhances due to the impact of radiation, which consequently produces the higher temperature in the viscous dominant region. The influences of hybrid nanoparticle volume fractions (φ_1, φ_2) on the temperature and velocity fields are depicted in Figs. 6 and 7, respectively. Fig. 6 explains that the velocity of nanofluid shrinks due to φ_1 and φ_2 in both results and so augments the velocity boundary-layer. Physically, the nanoparticle volume fractions added in declining viscosity of a convectional regular fluid, i.e. water in the current investigation. Therefore, the velocity boundary-layer enhances. The sketch in Fig. 7 suggests that the temperature distribution upsurges due to φ_1 and φ_2 in both solutions. Physically, hybrid nanomaterial dispersion enhances the thermal energy in the

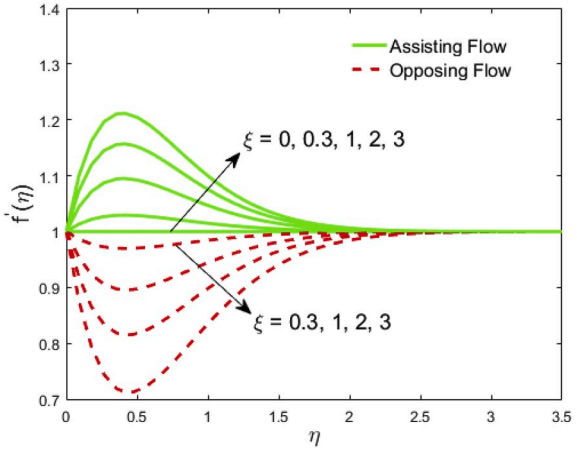

Fig. 8. Comparison of $f'(\eta)$ with Fig. 8 of Ishak et al. [42] when $\Pr = 1, m = \lambda = 1, S = \varepsilon = \varphi = M = 0$.

nanofluid hybrid layer which consequently increases nanofluid temperature. Accordingly, the current findings show that the utilization of hybrid nanomaterials can help us develop improved heat circulation in particular heat transfer equipment and can accumulate energy through chemical processes. Finally, Fig. 8 is prepared to validate our outcomes with graphical illustration of Ishak et al. [42]. Excellent accuracy is observed.

4. Conclusion

This current research endeavors to work out the problem of steady mixed convective radiative flow with heat transfer through an erratic variable thicker shrinking/stretching sheet involving hybrid water based (SiO_2–MoS_2) nanomaterials. The collocation technique, identified as bvp4c has been utilized to solve the problem in ODEs form. The vital points of the current investigation are given below:

- In the varying amount of the shrinking/stretching parameter, multiple solutions are found.
- Due to magnetic number, the velocity increases in the first branch solution, while the opposite impact is seen in the second branch solution.
- The temperature augments due to radiation in the both solutions.
- The nanoparticle volume fractions shrink the velocity of nanofluid and upsurge the temperature distribution in both solutions.

References

[1] A. Wakif, Z. Boulahia, S.R. Mishra, M.M. Rashidi, R. Sehaqui, Influence of a uniform transverse magnetic field on the thermo-hydrodynamic stability in water-based nanofluids with metallic nanoparticles using the generalized Buongiorno's mathematical model, Eur. Phys. J. Plus 133 (2018) 181.
[2] M. Sheikholeslami, R.U. Haq, A. Shafee, Z. Li, Y.G. Elaraki, I. Tlili, Heat transfer simulation of heat storage unit with nanoparticles and fins through a heat exchanger, Int. J. Heat Mass Tran. 135 (2019) 470–478.
[3] A. Wakif, I.L. Animasaun, N.P.V. Satya, G. Sarojamma, Meta-analysis on thermo-migration of tiny/nano-sized particles in the motion of various fluids, Chin. J. Phys. (2019), https://doi.org/10.1016/j.cjph.2019.12.002.
[4] A. Wakif, M. Qasim, M.I. Afridi, S. Saleem, M.M. Al-Qarni, Numerical examination of the entropic energy harvesting in a magnetohydrodynamic dissipative flow of Stokes' second problem: utilization of the gear-generalized differential quadrature method, J. Non-Equil. Thermody. 44 (2019) 385–403.
[5] M. Sheikholeslami, B. Rezaeianjouybari, M. Darzi, A. Shafee, Z. Li, T.K. Nguyen, Application of nano-refrigerant for boiling heat transfer enhancement employing an experimental study, Int. J. Heat Mass Tran. 141 (2019) 974–980.
[6] M.K. Nayak, A. Wakif, I.L. Animasaun, M.S.H. Alaoui, Numerical differential quadrature examination of steady mixed convection nanofluid flows over an isothermal thin needle conveying metallic and metallic oxide nanomaterials: a comparative investigation, Arabian J. Sci. Eng. (2020), https://doi.org/10.1007/s13369-020-04420-x.
[7] M. Sheikholeslami, M. Jafaryar, A. Shafee, H. Babazadeh, Acceleration of discharge process of clean energy storage unit with insertion of porous foam considering nanoparticle enhanced paraffin, J. Clean. Prod. 261 (2020) 121206.
[8] T. Thumma, A. Wakif, I.L. Animasaun, Generalized differential quadrature analysis of unsteady three-dimensional MHD radiating dissipative Casson fluid conveying tiny particles, Heat Transf (2020), https://doi.org/10.1002/htj.21736.
[9] A. Zaib, U. Khan, A. Wakif, M. Zaydan, Numerical entropic analysis of mixed MHD convective flows from a non-isothermal vertical flat plate for radiative tangent hyperbolic blood biofluids conveying magnetite ferroparticles: dual similarity solutions, Arabian J. Sci. Eng. (2020), https://doi.org/10.1007/s13369-020-04393-x.
[10] K. Niihara, New design concept of structural ceramics/ceramic nanocomposites, Nippon Seramikkusu Kyokai Gakujutsu Ronbunshi 99 (1991) 974–982.
[11] S. Jana, A. Salehi-Khojin, W.-H. Zhong, Enhancement of fluid thermal conductivity by the addition of single and hybrid nano-additives, Thermochim. Acta 462 (2007) 45–55.
[12] S. Suresh, K.P. Venkitaraj, P. Selvakumar, M. Chandrasekar, Synthesis of Al_2O_3–cu/water hybrid nanofluids using two step method and its thermo physical properties, Colloids Surf., A 388 (2011) 41–48.
[13] G.G. Momin, Experimental investigation of mixed convection with water-Al_2O_3 & hybrid nanofluid in inclined tube for laminar flow, Int. J. Sci. Technol. Res. 2 (2013) 195–202.
[14] S. Suresh, K.P. Venkitaraj, P. Selvakumar, M. Chandrasekar, Effect of Al_2O_3–cu/water hybrid nanofluid in heat transfer, Exp. Therm. Fluid Sci. 38 (2012) 54–60.

[15] M. Baghbanzadeh, A. Rashidi, D. Rashtchian, R. Lotfi, A. Amrollahi, Synthesis of spherical silica/multiwall carbon nanotubes hybrid nanostructures and investigation of thermal conductivity of related nanofluids, Thermochim. Acta 549 (2012) 87–94.
[16] N.S. Khashi'ie, N.M. Arifin, E.H. Hafidzuddin, N. Wahi, I. Pop, Mixed convective stagnation point flow of a thermally stratified hybrid Cu-Al_2O_3/water nanofluid over a permeable stretching/shrinking sheet, ASM Sc. J. 12 (5) (2019) 17–25. ICoAIMS2019.
[17] L.A. Lund, Z. Omar, I. Khan, E.M. Sherif, Dual solutions and stability analysis of a hybrid nanofluid over a stretching/shrinking sheet executing MHD flow, Symmetry 12 (2020) 276.
[18] A. Wakif, A.J. Chamkha, T. Thumma, I.L. Animasaun, R. Sehaqui, Thermal radiation and surface roughness effects on the thermo-magneto-hydrodynamic stability of alumina–copper oxide hybrid nanofluids utilizing the generalized Buongiorno's nanofluid model, J. Therm. Anal. Calorim. (2020), https://doi.org/10.1007/s10973-020-09488-z.
[19] M.S. Khan, I. Karim, M.S. Islam, M. Wahiduzzaman, MHD boundary layer radiative, heat generating and chemical reacting flow past a wedge moving in a nanofluid, Nano Convergence 1 (2014) 1–13.
[20] T. Poornima, N.B. Reddy, Radiation effects on MHD free convective boundary layer flow of nanofluids over a nonlinear stretching sheet, Adv. Appl. Sci. Res. 4 (2013) 190–202.
[21] N.A. Aini Mat, N.M. Arifin, R. Nazar, F. Ismail, N. Bachok, MHD mixed convection flow of a power law nanofluid over a vertical stretching sheet with radiation effect, AIP Conference Proceedings 1557 (2013) 604.
[22] S. Shateyi, J. Prakash, A New numerical approach for mhd laminar boundary layer flow and heat transfer of nanofluids over a moving surface in the presence of thermal radiation, Bound. Value Probl. 2 (2014) 1–12.
[23] M.G. Reddy, Influence of magnetohydrodynamic and thermal radiation boundary layer flow of a nanofluid past a stretching sheet, J. Sci. Res. 6 (2014) 257–272.
[24] E. Haile, B. Shankar, A Steady Mhd boundary-layer flow of water based nanofluids over a moving permeable flat plate, Int. J. Math. Res. 4 (2014) 27–41.
[25] A. Shafiq, I. Khan, G. Rasool, A.H. Seikh, El-Sayed M. Sherif, Significance of double stratification in stagnation point flow of third-grade fluid towards a radiative stretching cylinder, Mathematics 7 (11) (2019) 1103.
[26] A. Shafiq, Z. Hammouch, Hakan F. Oztop, Radiative MHD flow of third-grade fluid towards a stretched cylinder. International Conference on Computational Mathematics and Engineering Sciences, Springer, Cham, 2019, pp. 166–185.
[27] G. Rasool, A. Shafiq, I. Tlili, Marangoni convective nanofluid flow over an electromagnetic actuator in the presence of first-order chemical reaction, Heat Tran. Asian Res. 49 (1) (2020) 274–288.
[28] G. Rasool, T. Zhang, Characteristics of chemical reaction and convective boundary conditions in Powell-Eyring nanofluid flow along a radiative Riga plate, Heliyon 5 (4) (2019), e01479.
[29] A. Shafiq, I. Zari, G. Rasool, I. Tlili, T.S. Khan, On the MHD Casson axisymmetric Marangoni forced convective flow of nanofluids, Mathematics 7 (11) (2019) 1087.
[30] A. Wakif, A novel numerical procedure for simulating steady MHD convective flows of radiative Casson fluids over a horizontal stretching sheet with irregular geometry under the combined influence of temperature-dependent viscosity and thermal conductivity, Math. Probl Eng. 2020 (2020) 1–20.
[31] W.A. Khan, I. Haq, M. Ali, M. Shahzad, M. Khan, M. Irfan, Significance of static-moving wedge for unsteady Falkner–Skan forced convective flow of MHD cross fluid, J. Braz. Soc. Mech. Sci. Eng. 40 (2018) 470.
[32] A.S. Dogonchi, S.M. Seyyedi, M.H. Tilehnoee, A.J. Chamkha, D.D. Ganji, Investigation of natural convection of magnetic nanofluid in an enclosure with a porous medium considering Brownian motion, Case Stud. Therm. Eng. 14 (2019) 100502.
[33] M. Waqas, M.M. Gulzar, W.A. Khan, M.I. Khan, N.B. Khan, Newtonian heat and mass conditions impact in thermally radiated Maxwell nanofluid Darcy-Forchheimer flow with heat generation, Int. J. Numer. Methods Heat Fluid Flow 29 (2019) 2809–2821.
[34] U. Khan, A. Zaib, Z. Shah, D. Baleanu, El S. M-Sherif, Impact of magnetic field on boundary-layer flow of Sisko liquid comprising nanomaterials migration through radially shrinking/stretching surface with zero mass flux, J. Mater. Res. Technol. (2020), https://doi.org/10.1016/j.jmrt.2020.01.107.
[35] H. Xie, B. Jiang, B. Liu, Q. Wang, J. Xu, F. Pan, An investigation on the tribological performances of the SiO_2-MoS_2 hybrid nanofluids for magnesium alloy-steel contacts, Nano. Res. Lett. 11 (2016) 329–336.
[36] U. Khan, A. Zaib, I. Khan, D. Baleanu, K.S. Nisar, Enhanced heat transfer in moderately ionized liquid due to hybrid MoS_2/SiO_2 nanofluids exposed by nonlinear radiation: stability analysis, Crystals 10 (2020) 142.
[37] E.N. Maraj, Z. Iqbal, E. Azhar, Z. Mehmood, A comprehensive shape factor analysis using transportation of MoS_2-SiO_2/H_2O inside an isothermal semi vertical inverted cone with porous boundary, Result Phys 8 (2018) 633–641.
[38] M.N. Rostami, S. Dinarvand, I. Pop, Dual solutions for mixed convective stagnation-point flow of an aqueous silica-alumina hybrid nanofluid, Chin. J. Phys. 56 (5) (2018) 2465–2478.
[39] S.S. Ghadikolaei, M. Gholinia, M.E. Hoseini, D.D. Ganji, Natural convection MHD flow due to MoS_2 –Ag nanoparticles suspended in $C_2H_6O_2$–H_2O hybrid base fluid with thermal radiation, J. Taiwan Inst. Chem. Eng. 97 (2019) 12–23.
[40] T.R. Mahapatra, A.S. Gupta, Heat transfer in stagnation-point flow towards a stretching sheet, Heat Mass Tran. 38 (6) (2002) 517–521.
[41] R. Nazar, A. Norsarahaida, D. Filip, I. Pop, Unsteady boundary layer flow in the region of the stagnation point on a stretching sheet, Int. J. Eng. Sci. 42 (11–12) (2004) 1241–1253.
[42] A. Ishak, R. Nazar, I. Pop, Mixed convection boundary layers in the stagnation-point flow toward a stretching vertical sheet, Meccanica 41 (2006) 509–518.